

Long QT syndrome, Brugada syndrome, and conduction system disease are linked to a single sodium channel mutation

See the related Commentary beginning on page 1075.

Augustus O. Grant,¹ Michael P. Carboni,¹ Valentina Neplioueva,¹ C. Frank Starmer,² Mirella Memmi,³ Carlo Napolitano,³ and Silvia Priori³

¹Duke University Medical Center, Durham, North Carolina, USA

²Medical University of South Carolina, Charleston, South Carolina, USA

³Instituto di Recovero e Cura a Carattere Scientifico, Fondazione Salvatori Maugeri, University of Pavia, Pavia, Italy

The function of the 12 positive charges in the 53-residue III/IV interdomain linker of the cardiac Na⁺ channel is unclear. We have identified a four-generation family, including 17 gene carriers with long QT syndrome, Brugada syndrome, and conduction system disease with deletion of lysine 1500 (Δ K1500) within the linker. Three family members died suddenly. We have examined the functional consequences of this mutation by measuring whole-cell and single-channel currents in 293-EBNA cells expressing the wild-type and Δ K1500 mutant channel. The mutation shifted the potential for half inactivation ($V_{1/2h_{\infty}}$) to more negative values and reduced its voltage dependence consistent with a reduction of inactivation valence of 1. The shift in inactivation was the result of an increase in closed-state inactivation rate (11-fold at -100 mV). The potential for half activation ($V_{1/2m}$) was shifted to more positive potentials, and its voltage dependence reduced by 50% in the Δ K1500 mutant. To determine whether the positive charge deletion was the basis for the gating changes, we performed the mutations K1500Q and K1500E (Δ charge, -1 , -2). For both mutations, $V_{1/2h_{\infty}}$ was shifted back toward control; however, $V_{1/2m}$ shifted progressively to more positive potentials. The late component of Na⁺ current was increased in the Δ K1500 mutant channel. These changes can account for the complex phenotype in this kindred and point to an important role of the III/IV linker in channel activation.

J. Clin. Invest. 110:1201–1209 (2002). doi:10.1172/JCI200215570.

Introduction

The inward Na⁺ current sustains propagation in the atrium, ventricle, and His-Purkinje system. Mutations in the cardiac Na⁺ channel α subunit gene Na_v1.5 have been associated with a spectrum of clinical rhythm disorders, including long QT syndrome, type 3 (LQT3), Brugada syndrome, and progressive cardiac conduction system disease (PCCD) (1–3). The wild-type Na⁺ channel usually opens once or twice during depolarization and then enters a fast-inactivated state, rarely returning to the open state during maintained depolarization. In LQT3, the inactivated state is destabilized, and late return to the open state is more frequent (4). This late component of inward current prolongs the action potential duration and the QT interval on

the surface electrocardiogram (EKG) and increases the likelihood of spontaneous oscillations of membrane potential. The LQT3 mutations tend to cluster around the III/IV interdomain linker, the neighboring segments of domains III and IV, and the carboxy-terminus (5). Mutations that reduce the magnitude of the Na⁺ current result in Brugada syndrome and PCCD (2, 6, 7). The Brugada syndrome mutations exaggerate the normal epicardial-to-endocardial potential gradient that is most prominent at the base of the right ventricle. The resulting heterogeneity of repolarization produces ST segment elevation in the right precordial leads, and phase 2 re-entry (8). Conduction disturbance is a part of this syndrome, as the HV interval is frequently prolonged (9). In the only PCCD mutation that has been functionally expressed, competing gating effects result in conduction slowing without the ST-T wave changes characteristic of Brugada syndrome (10).

Recent studies suggest significant overlap in phenotype (11, 12). Individuals with the same mutation may have LQT3 or the Brugada phenotype. Administration of Na⁺ channel-blocking drugs to patients with LQT3 may precipitate EKG changes characteristic of Brugada syndrome (13). We have identified a four-generation kindred including 17 gene carriers and four instances of sudden death. Members of the kindred had all three

Received for publication March 29, 2002, and accepted in revised form July 30, 2002.

Address correspondence to: Augustus O. Grant, Box 3504, Duke Medical Center, Durham, North Carolina 27710, USA. Phone: (919) 684-3901; Fax: (919) 681-8978; E-mail: grant007@mc.duke.edu.

Conflict of interest: No conflict of interest has been declared.

Nonstandard abbreviations used: progressive cardiac conduction system disease (PCCD); long QT syndrome, type 3 (LQT3); electrocardiogram (EKG); protein kinase C-dependent (PKC-dependent); long QT syndrome (LQTS); ventricular fibrillation (VF); right ventricular (RV).

phenotypes: LQT3, Brugada syndrome, and widespread, profound conduction system disturbances, including in the sino-atrial region. Individuals with long QT syndrome, Brugada system, or conduction system disease had a single amino acid deletion, K1500, in the III/IV interdomain linker. A missense mutation at the same site, K1500N, was considered nonpathogenic (14). The K1500 residue is one of the 12 positively charged amino acids in the 53-residue III/IV interdomain linker. Five negative charges are also present in the linker. This charge density is similar to that in the S4 segment of each homologous domain, a channel region critical for activation gating. K1500 forms part of a helically structured region of the inactivation gate (15). K1500 is only five residues from the lysine residue in the LQT3-associated mutation Δ KPQ. The more widespread functional disturbance in the K1500 mutation (hereafter referred as Δ K1500) compared with the three-residue deletion Δ KPQ suggests a functionally important role of K1500. This residue also forms a part of the consensus sequence for protein kinase C-dependent (PKC-dependent) phosphorylation of the Na⁺ channel. PKC-dependent phosphorylation is required for PKA-dependent modulation of the Na⁺ channel (16).

We have expressed Δ K1500 and related mutations K1500E, K1500Q, and Δ K1499 in 293-EBNA cells. The functional disturbances in channel gating can account for all three phenotypic variants of the mutation. The studies suggest a more specific role for the charged residues of the III/IV interdomain linker in Na⁺ channel activation.

Methods

Clinical presentations. A 13-year-old boy (IV-13; Figure 1) came to our attention after an EKG recording obtained prior to sports participation showed a prolonged QT interval (QTc 510 ms; Figure 2). The morphology of the QT interval was suggestive of an LQT3 variant (17). Molecular screening of the genes related to long QT syndrome (LQTS) demonstrated the presence of a single amino acid deletion (Δ K1500) in the III/IV interdomain linker of the Na_v 1.5 gene. The boy was asymptomatic, but the family history revealed that sudden cardiac deaths with negative autopsy examinations had occurred in two male subjects aged 49 and 19 years (II-6 and IV-1, respectively; Figure 1). This finding prompted a clinical and genetic evaluation of all family members. The father of the proband (III-14; Figure 1) had a prolonged QT interval (QTc 480 ms). He had experienced several syncopal episodes, and during one of these, first-degree atrioventricular block and asystole had been observed (Figure 2); therefore he had received a pacemaker at the age of 59 years. DNA analysis confirmed the presence of the K1500 deletion mutation.

The proband's 61-year-old paternal uncle (III-12; Figure 1), that uncle's 30-year-old son (IV-12; Figure 1), and that son's 2-year-old son (V-5; Figure 1) also carried the mutation within the Na_v 1.5 gene. III-12 had a clinical history of syncopal events that occurred when he was in

his thirties; he had been hospitalized, but no cause for the fainting episodes had been identified. An EKG recorded in 1968 showed ST segment elevation in leads V1–V3; however, this pattern was not present during the resting EKG at the time of the clinical evaluation. A challenge with flecainide (2 mg/kg intravenously) induced ST segment elevation with the “coved-type” morphology (18). The subject coded as IV-12, the son of III-12, was asymptomatic; his EKG was normal, but a flecainide challenge unmasked a Brugada-like EKG. A Holter recording demonstrated the presence of sinus pauses greater than 4 seconds occurring at rest that were not associated with the symptoms. The patient underwent programmed electrical stimulation, and ventricular fibrillation (VF) was induced after delivery of 2 premature extrastimuli from the right ventricular (RV) outflow tract. An implantable cardioverter defibrillator was implanted in the patient. The 2-year-old son of IV-12 (V-5; Figure 1) had a normal EKG, and no further investigation was performed.

Three paternal cousins of III-14, sons and a daughter of one of the victims of cardiac arrest, were identified as carriers of the Na_v 1.5 mutation (III-5, III-7, and III-10; Figure 1). Evaluation of their descendants identified eight additional mutation carriers, four of whom had a history of syncopal events of unknown etiology. Seven individuals presented with a prolonged QT interval (i.e., QTc > 460 ms), and typical ST segment elevation was unmasked in six when the flecainide test was performed. Additionally, one subject (IV-3; Figure 1) presented with a PR interval at the upper limit of normal, complete right bundle branch block, and sinus pauses associated with fainting (Figure 2). Two individuals with a history of presyncopal events (IV-2 and IV-3) agreed to undergo programmed electrical stimulations. In each of these individuals, VF was inducible with two premature stimuli from the RV apex. An implantable cardioverter defibrillator was implanted in each. After 3 years of follow-up, VF was inducible in none of the three individuals in whom we performed programmed electrical stimulation, none had experienced cardiac events, and the Holter function of the implantable cardioverter defibrillator failed to document sustained cardiac arrhythmias.

III-14's asymptomatic paternal cousin III-2, whose brother (III-1) died suddenly at age 55 (Figure 1), elected to undergo genetic analysis but refused clinical evaluation after she was diagnosed as a carrier of the mutation (Figure 1). For the kindred, a lod score of 3.61 was obtained using a marker on locus 3p21, $\theta = 0.01$.

Preparation of cell lines expressing the wild-type and mutant Na⁺ channels. The K1500 deletion, K1500E, K1500Q, and Δ K1499 mutations of the Na⁺ channel gene Na_v 1.5 were performed using recombinant PCR (19). Fidelity of the mutations was documented by direct sequencing. Human embryonic kidney cells (293-EBNA) were transfected with the plasmids pcDNA3.1/hH1, pcDNA3.1/hH1 Δ K1500,1499, pcDNA3.1/hH1K1500E,

and pcDNA3.1/hH1K1500Q using lipofectamine. Stable cell lines were established in 293-EBNA cells using hygromycin as the dominant selective marker.

Experimental setup. Whole-cell and single Na⁺ channel currents were measured using standard patch-clamp techniques (20). Cells were superfused with a 130-mM Na⁺ external solution for the whole-cell recordings. The 0.5- to 1.5-MΩ micropipettes were filled with an internal CsCl solution. The internal Cs⁺ blocked the endogenous K⁺ channels in the HEK-293 EBNA cells. Under these recording conditions, the inward Na⁺ current was the only ionic current recorded. Cells were superfused with a high potassium-aspartate solution for single-channel recordings. The high-potassium solution reduced the membrane potential to approximately 0 mV. Membrane potentials are reported as absolute values (i.e., referenced to 0 mV). The 10- to 20-MΩ micropipettes were filled with a Na⁺ external solution. In occasional patches, we observed outward single-channel currents that were kinetically distinct from the Na⁺ channels. Trials with such activity were excluded from analysis.

Solutions. The solutions used in these experiments had the following compositions (mM): Na⁺ external solution: NaCl 130, KCl 4, CaCl₂ 1, MgCl₂ 5, HEPES

5, glucose 5 (pH adjusted to 7.4 with NaOH); Cs⁺ micropipette solution: CsCl 130, MgCl₂ 1, MgATP 5, 1,2-bis (aminophenoxy) ethane-N,N,N',N'-tetraacetic acid 10, HEPES 10 (pH adjusted to 7.2 with CsOH); high-potassium external solution: potassium-aspartate 140, KCl 10, MgCl₂ 2, CaCl₂ 1, glucose 5, HEPES 5 (pH adjusted to 7.4 with KOH); Na⁺ micropipette solution for single-channel recordings: NaCl 140, KCl 5, MgCl₂ 2.5, CaCl₂ 0.5, HEPES 5 (pH adjusted to 7.4 with NaOH). All experiments were performed at room temperature (20–22 °C).

Recording techniques. We recorded whole-cell and single-channel currents using an Axopatch-200A (Axon Instruments Inc., Burlingame, California, USA) or EPC-7 (List Medical, Darmstadt, Germany) patch-clamp amplifier. The tip of each micropipette was coated with a hydrophobic electrometer. Series resistance and capacity transient were compensated using standard techniques. At the beginning of each experiment, adequacy of voltage control was assessed as previously described (21). Whole-cell currents were filtered at 10 kHz and digitized at 20–40 kHz.

We recorded single-channel current with high-resistance (10–20 MΩ) microelectrodes. To compare open times, we reduced the holding potential to decrease the

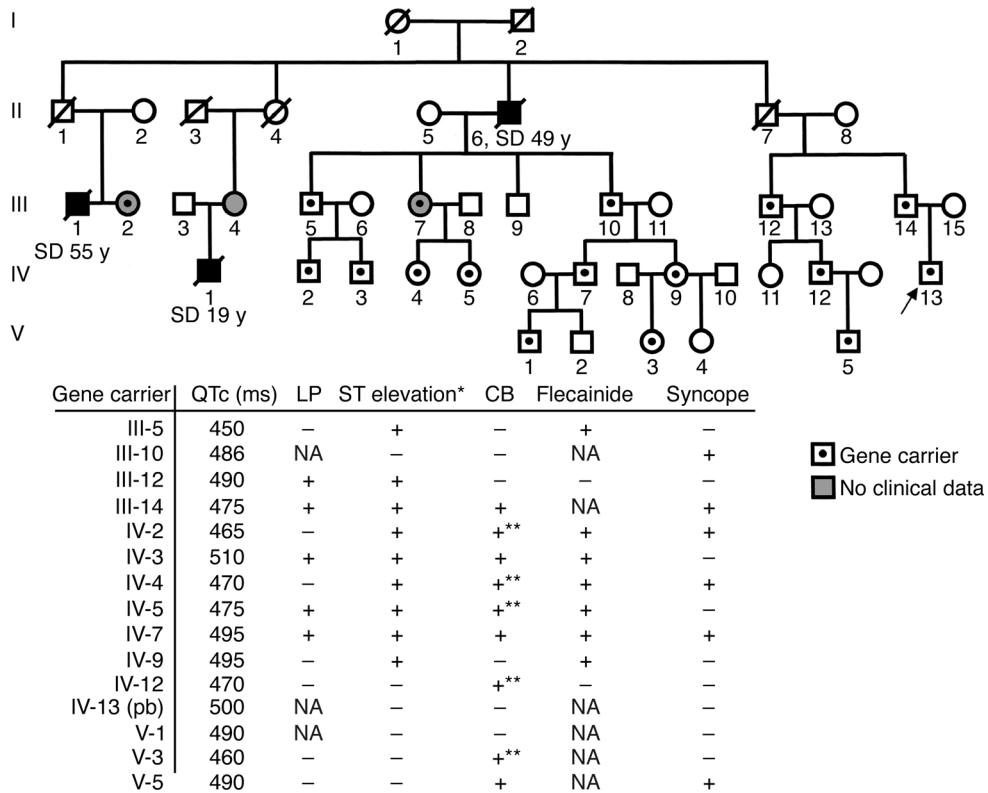


Figure 1

A pedigree of the family and a summary of the different cardiac phenotypes observed in the 15 genetically affected individuals who were clinically investigated. Overall, in this family, three pathological phenotypes have been associated with the Na_v1.5 K1500 deletion mutation (Figure 2): QT interval prolongation, ST segment elevation in V1–V3 (with the typical Brugada-like morphology), and conduction abnormalities. Forty percent of gene carriers reported syncopal episodes in their clinical history, and in two of them these episodes were related to sinus pauses. LP, late potential; CB, conduction block; pb, proband; SD, sudden death. *Spontaneous ST segment elevation in V1–V3. **Incomplete right bundle branch block.

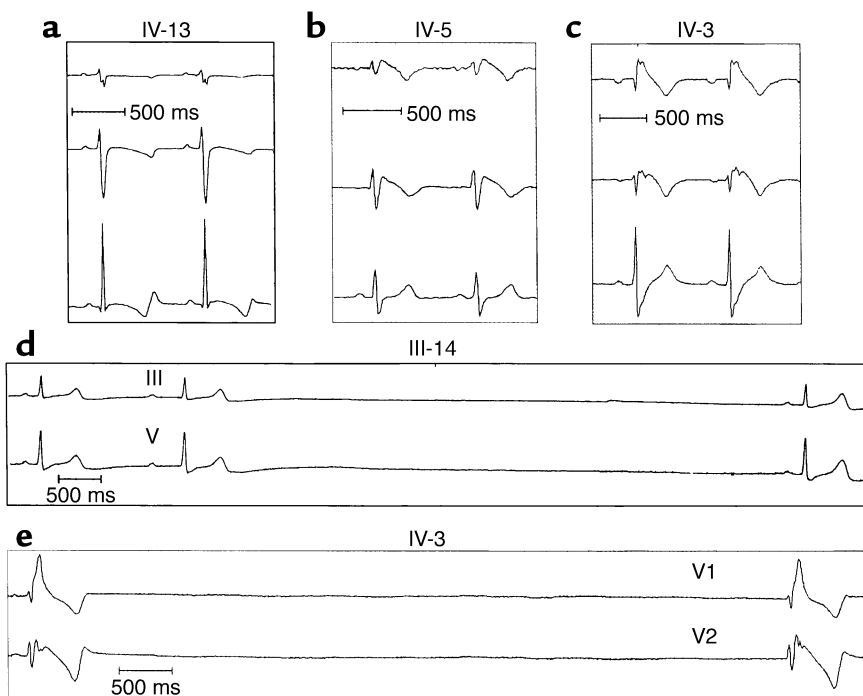


Figure 2
EKG traces of mutation carriers showing leads V1, V2, and V5. (a) QT interval prolongation (patient IV-13 of the pedigree shown in Figure 1). (b) ST segment elevation (patient IV-5 of the pedigree). (c) ST segment elevation and right bundle branch block (patient IV-3 of the pedigree). (d) First-degree AV block and sinus arrest (patient III-14 of the pedigree). (e) Right bundle to branch block and prolonged sinus pause.

number of overlapping events (less than four) at the test potential of -20 mV. Experiments involving analysis of the late Na^+ currents were recorded with 5- to 10-M Ω microelectrodes to increase the number of channels in the patch. The holding potential was set at -100 to -80 mV. Two-hundred-millisecond test pulses were applied to -40 and -20 mV. Currents were filtered at 2.5 kHz and digitized at 20 kHz.

Data analysis. Whole-cell and single-channel currents were analyzed with custom software developed in our laboratory (21, 22). Availability-voltage and activation-voltage relationships were fit to a standard Boltzmann equation: $h_{\infty}, m_{\infty} = 1 / \{1 + \exp[(V - V_{1/2}) / k]\}$, where h_{∞} is the inactivation variable, m_{∞} the activation variable, V the membrane potential, $V_{1/2}$ the potential at which h_{∞} or $m_{\infty} = 0.5$, and k the slope factor.

The development and recovery from inactivation were fit with a single exponential function: $I(t) = I_{\infty} [1 - \exp(-t/\tau)]$, where $I(t)$ is the current at time t , I_{∞} the initial current or the steady-state current, and τ the inactivation time constant.

To study the late component of the whole-cell current, recordings were performed at high gain ($\times 2$ to $\times 5$) and the leakage current was subtracted using scaled averaged currents to a test potential of -80 mV. The leakage and capacity transient of the single-channel current were reduced by subtraction. Current trials were scanned, and null sweeps were averaged and subtracted from each trial. The base-line and single-channel amplitude were determined from the histogram of digitized currents. The single-channel detection threshold was set at $0.5 \times$ the single current amplitude. The open-time histogram was fit to a single exponential function.

Values are reported as means \pm SE, unless otherwise stated. Comparisons were made with unpaired or paired t tests, or ANOVA, as appropriate.

Results

The wild-type and ΔK1500 , K1500E, K1500Q, and ΔK1499 mutant α subunits expressed current of several nanoamperes in the 293-EBNA cells. Initially, we determined the equilibrium gating parameters of the cells expressing the wild-type and spontaneous mutant channels. Availability- and activation-voltage relationships of the wild-type and ΔK1500 are summarized in Figure 3. $V_{1/2h}$ was shifted from -84.5 ± 1.3 mV ($n = 9$) in the wild-type to -97.9 ± 1 mV ($n = 13$) in the ΔK1500 mutant. The slope factor was increased from 4.8 ± 0.1 to 6.2 ± 0.1 mV. The shift in $V_{1/2h}$ reduced h_{∞} from 0.72 in the wild-type to 0.23 in the ΔK1500 mutant at the normal resting potential of a ventricular cell, resulting in a loss of function. The activation-voltage relationship was shifted in the opposite direction: $V_{1/2m}$ decreased from -47 ± 1.5 to -44 ± 0.3 mV. The slope factor was almost doubled: 7.5 ± 0.4 mV in the wild-type and 13 ± 0.3 mV in the ΔK1500 mutant. The shifts in gating parameters were significant. Representative current recordings are presented in Figure 3, c-f.

In some Brugada syndrome mutations, the negative shift in Na^+ channel availability is associated with substantial use-dependent reduction in current during pulse-train stimulation (12, 23). We examined the effect 40-ms pulses applied from -100 to -20 mV at various cycle lengths. The results at a cycle length of 90 ms are summarized in Figure 4a; currents from one experiment are illustrated in Figure 4b. Despite a steady-state availability of only 0.58 at -100 mV, we observed no

use-dependent reduction in Na⁺ current with the ΔK1500 mutant. We performed four additional experiments with trains of 100-ms pulses (cycle length 150 ms) and observed similar results (currents from one experiment are illustrated in Figure 4c). The results suggest that recovery from inactivation must be extremely rapid in the ΔK1500 mutant channel. Two measures of Na⁺ channel inactivation are presented in Figure 5. Measurements obtained with conditioning and test pulse sequences are presented in Figure 5a; those obtained from single exponential fits to the whole-cell current relaxation are presented in Figure 5b. At conditioning potentials of -140, -120, and -100 mV, the time constant of recovery from inactivation was determined by application of twenty 40-ms pulses from the conditioning potential to -20 mV. At a conditioning potential of -90 mV, we used a single 40-ms pulse to -20 mV. After a variable recovery interval, a test pulse to -20 mV was applied. The test pulse current was plotted as a function of the recovery intervals. Time constants derived from single exponential fits to the recovery process are plotted in Figure 5a. At conditioning potentials of -80, -70, and -60 mV, the development of inactivation was assessed by a single pulse of variable duration to the respective conditioning potential, followed by a test pulse to -20 mV. The peak test pulse current was plotted against the duration of the conditioning pulse, and the time constant of development of inactivation was determined from single exponential fits. These time constants are also plotted in Figure 5a. The bell-shaped relationship between the wild-type time constant and *V* was similar to that observed by others in these cells (24). The time constant, τ , is small at -140 mV and reaches a relative maximum at -80 mV; the dynamic change τ_{-80}/τ_{-140} was 2.9. The voltage-dependence of τ for the ΔK1500 mutant was substantially less. The dynamic change was only 1.3.

The relaxation of the macroscopic current provides another measure of channel inactivation. At potentials negative to approximately -40 mV, the first latency distribution, deactivation and inactivation rates influence the macroscopic current relaxation (25, 26). At potentials positive to -20 mV, the macroscopic relaxation reflects the rate of inactivation. As Figure 5b illustrates, overall inactivation rate is less voltage-dependent in the ΔK1500 mutant than in the wild-type. Although the inactivation rate is faster in ΔK1500 at hyperpolarized potentials, there is a crossover at -40 mV, with the relaxation rate of the wild-type exceeding that of the ΔK1500 mutant.

The inactivation kinetics must account for the observation that τ is smaller in ΔK1500 at potentials positive to -120 mV, yet h_{∞} is small. This suggests that the mutation must be associated with a marked increase in the rate of onset of macroscopic inactivation. The inactivation rate constants α_h and β_h are related to τ and h_{∞} by the following relationships: $\tau = 1/(\alpha_h + \beta_h)$; $h_{\infty} = \alpha_h/(\alpha_h + \beta_h)$. From the measurements of τ and h_{∞} , we estimated α_h and β_h . Whereas the rate of recovery from

inactivation, α_h , was similar in the wild-type and ΔK1500 channels (80/s and 61/s, respectively), β_h was increased 11-fold in the mutant.

The substantial increase in the onset rate of inactivation in the ΔK1500 mutant and the reduction in slope factor (equivalent to the loss of one electronic charge, ϵ_0) suggested that K1500 plays a critical role in channel inactivation. According to current Na⁺ channel gating models, activation is associated with a $12\epsilon_0$ outward movement of positive charges from S4 (27). The III/IV interdomain linker then moves into the pore to close the channel. The positive charges in the III/IV linker may set up repulsive forces with charges similar to those in S4 while the channel is closed and during the early phase of activation. The delayed outward movement of the inactivation would permit Na⁺ influx and delay channel closure. Otherwise the almost instantaneous closure of the channel would result in little measurable current. The faster inactivation onset in

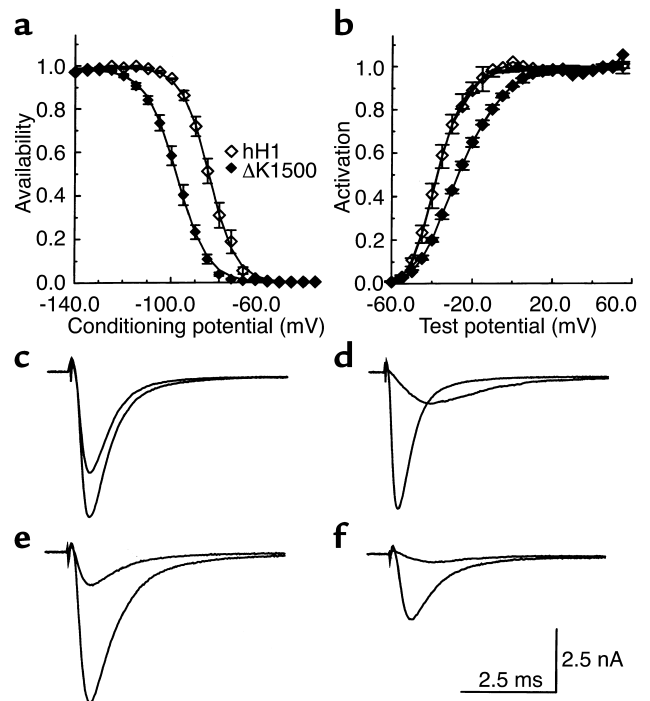


Figure 3 Shifts in gating kinetics associated with the ΔK1500 mutant. (a) Na⁺ channel availability was determined with 500-ms pulses to various potentials followed by test pulses to -20 mV. Test pulse currents were normalized and plotted against the conditioning potential. Gating parameters were obtained from fits with Boltzmann functions. $V_{1/2h}$ was -84.5 ± 1.3 mV ($n = 9$) for the wild-type and -97.9 ± 1 mV ($n = 13$) for the ΔK1500 mutant; the slope factor was 4.8 ± 0.1 and 6.2 ± 0.1 mV, respectively. (b) Activation currents were obtained with test pulses from a holding potential of -100 mV. $V_{1/2h}$ was -47.5 ± 1.5 mV for the wild-type and 49.5 ± 0.3 mV for the ΔK1500; slope factor was 7.5 ± 0.4 and 13 ± 0.3 mV, respectively. (c-f) Representative current recordings from cells expressing the wild-type (c and d) and ΔK1500 mutant channel (e and f). (c and e) Current obtained at a test potential of -20 mV after conditioning depolarizations to -140 and -90 mV. (d and f) Currents obtained at test potentials of -40 and -20 mV from a holding potential of -100 mV.

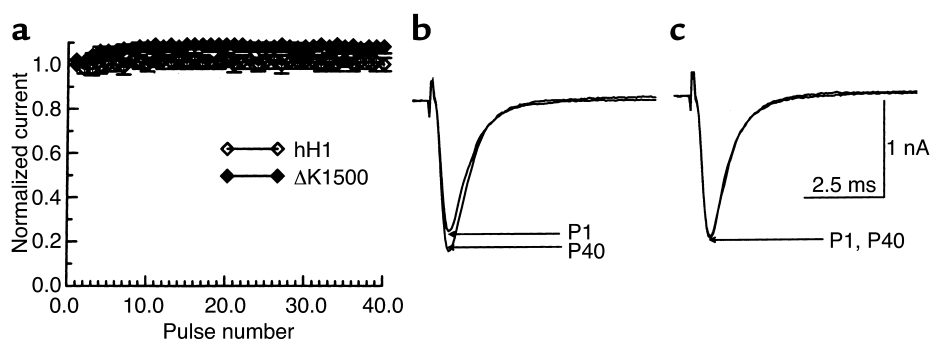


Figure 4

Na⁺ currents during pulse-train stimulation in the wild-type and ΔK1500 mutant Na⁺ channels. Trains of 40-ms pulses were applied from a holding potential of -100 mV to a test potential of -20 mV. (a) Normalized currents are plotted against pulse number. The interval between pulses was 50 ms (cycle length 90 ms). The data are from four experiments with the wild-type channel and ten with the ΔK1500 mutant. (b) Currents obtained with the ΔK1500 mutant channel using 40-ms pulses. (c) The results of one of four additional experiments with the ΔK1500 mutant using 100-ms pulses with 50-ms recovery intervals (cycle length 150 ms). P1, first pulse of train; P40, 40th pulse of train.

ΔK1500 (loss of one positive charge) would be consistent with this model. To test this hypothesis, we performed the mutation K1500E, resulting in a change in charge of -2. An interdomain III/IV-S4 repulsion model would predict even faster inactivation for the K1500E mutant. The gating parameters for wild-type, ΔK1500, and K1500E are summarized in Figure 6. The K1500E mutation shifted $V_{1/2h}$ back toward the control. However, there was a further 10-mV shift of $V_{1/2m}$ to -34.5 ± 0.9 mV. The charge substitution has a more predictable effect on activation than on inactivation. The results suggest that the negative shift in $V_{1/2h}$ and faster inactivation of the ΔK1500 mutant may result from either a reduction in the length of the III/IV interdomain linker or a change in the activation-inactivation coupling. Our initial studies with the ΔK1499 mutant gave a $V_{1/2h}$ of -92 ± 1.6 mV ($n = 6$). This suggests that the length of the linker is important in the negative shift. We investigated the effect of restoration of the chain length by performing the K1500Q mutation. This mutation has the same chain length as the wild-type channel and, like the ΔK1500 mutation, is associated with a charge change of -1. $V_{1/2}$ for inactivation of the K1500Q mutant channel was not different from that of the wild-type: -83.2 ± 0.8 mV ($n = 6$) versus -84.5 ± 1.3 mV ($n = 9$), respectively. However, like that of ΔK1500, $V_{1/2}$ for activation of K1500Q was shifted to more positive potentials: -38.3 ± 0.8 mV ($n = 6$) versus -47 ± 1.5 mV for the wild-type ($n = 9$). These results further support the conclusion that the primary role of K1500 is in channel activation.

The small difference in the relaxation rate of the macroscopic current (time constant of relaxation ≤ 1 ms) (Figure 5b) is unlikely to account for the QT interval prolongation observed in the affected family. To determine whether a late component of Na⁺ current might account for the QT interval prolongation, we recorded whole-cell currents with 200-ms pulses at high gain in cells expressing wild-type and ΔK1500 mutant channels. Figure 7 illustrates results from experiments in cells expressing each channel type. At 100 ms, the

persistent current amounted to 0.4% of the peak current in the wild-type and 1.5% in the ΔK1500. Summary data are presented in Figure 7c (hH1, $n = 4$; ΔK1500, $n = 5$). The ΔK1500 mutation was associated with a threefold increase in the late component of Na⁺ current.

Single-channel studies. The large negative shift of $V_{1/2h}$ in the ΔK1500 mutant channels might result entirely from an enhancement of closed-state inactivation. It is not clear whether open-state inactivation is also affected. Prior studies suggested that the triplet isoleucine, phenylalanine, methionine located in the III/IV interdomain linker controlled open-state inactivation. We examined the effect of the ΔK1500 mutation on open-state inactivation by recording single-Na⁺ channel currents in cell-attached membrane patches.

In one protocol, we used high-resistance microelectrodes and reduced the membrane potential in order to

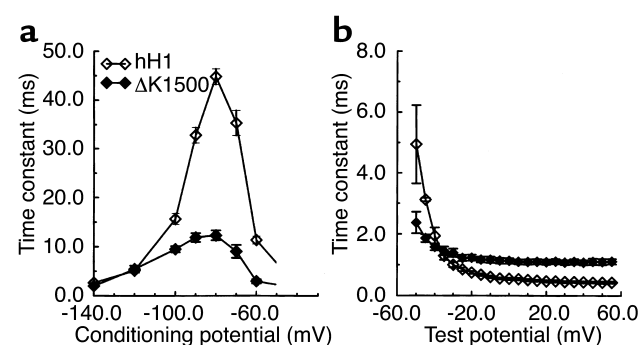


Figure 5

Voltage-dependence of Na⁺ channel inactivation. (a) Inactivation time constants were obtained with a protocol of conditioning and test pulses and plotted against conditioning voltage ($n = 6-8$ for hH1; $n = 3-9$ for ΔK1500). At potentials of -140, -120, and -100 mV, conditioning was effected by trains of twenty 40-ms pulses to -20 mV, followed by 20-ms test pulses. At potentials of -90, -80, -70, and -60 mV, a single conditioning pulse preceded each test pulse. (b) The relaxation phase of the Na⁺ current was fit with a single exponential function and plotted against the test potential ($n = 10$ for hH1; $n = 11$ for ΔK1500). Both measures show a reduction in the voltage-dependence of inactivation in the ΔK1500 mutant channels.

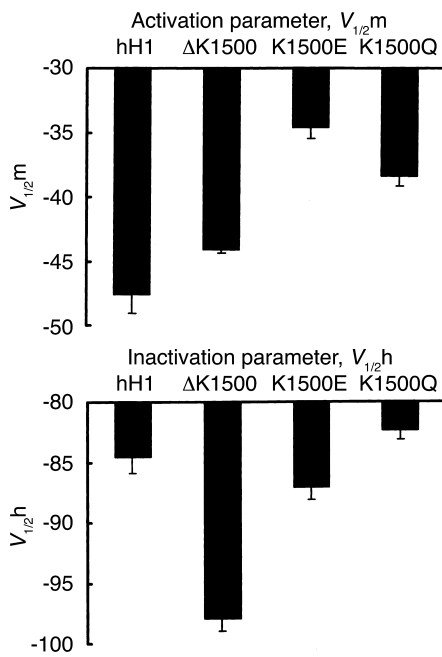


Figure 6

Inactivation and activation gating parameters in cells expressing the wild-type, Δ K1500, K1500E, and K1500Q mutant Na^+ channels. Inactivation and activation were determined with standard voltage clamp protocols. The values for m_∞ and h_∞ are the means of 9, 13, 12, and 6 experiments for hH1, Δ K1500, K1500E, and K1500Q, respectively. $V_{1/2m}$ for hH1 was significantly different from $V_{1/2m}$ for K1500E and K1500Q. $V_{1/2h}$ for Δ K1500 was significantly different from $V_{1/2h}$ for hH1, K1500E, and K1500Q. The bars represent SEM.

limit the number of overlapping events. Single-channel current amplitude was similar in the two channel types (1.4 ± 0.1 and 1.55 ± 0.05 pA; $n = 4$ for both hH1 and Δ K1500). However, the mean open time was significantly reduced in the Δ K1500 mutant (0.66 ± 0.02 ms in the wild-type vs. 0.56 ± 0.03 ms in the Δ K1500 mutant, $P < 0.05$). This result indicated that the Δ K1500 mutation also increased open-channel closure rate. At -20 mV, channels closed primarily by inactivation (25, 26).

Figure 7, d and e, compares single-channel currents recorded with low-resistance microelectrodes in wild-type and Δ K1500 mutant channels. The larger microelectrode tip allowed recordings from patches containing approximately 20 channels. Such recordings permitted the analysis of uncommon events, such as late opening of Na^+ channels, using a relatively small number of depolarizing trials. The first four trials in Figure 7, d and e, show currents recorded at -20 mV with 200-ms pulses. The lowest trace in each panel shows the currents obtained by averaging 499 wild-type trials and 300 Δ K1500 trials. The numbers of channels

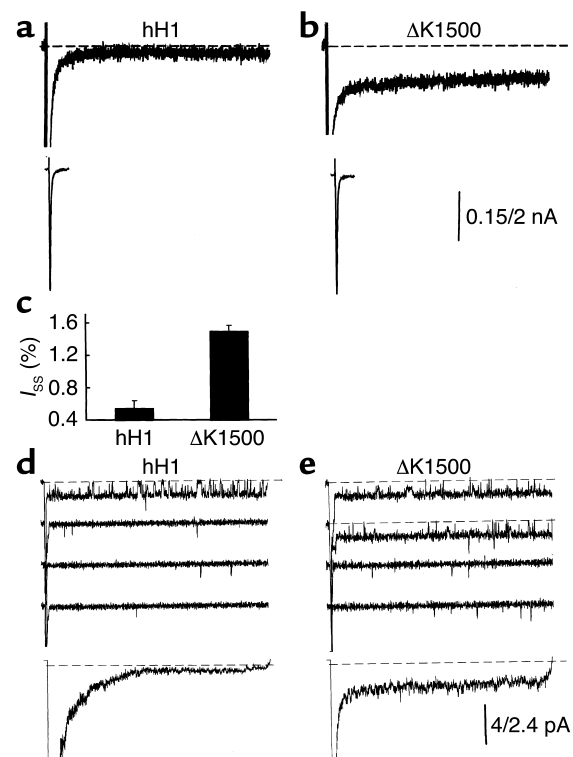
in the patch, estimated from recordings obtained at low gain, were 14 (wild-type) and 16 (Δ K1500). These estimates are at the lower limit, since the probability that a channel will open during a trial is always less than 1. The initial inward current saturated the amplifier and was truncated, as shown in Figure 7, d and e. At late times (operationally defined as $t > 20$ ms), currents consisting of isolated brief openings as well as bursts of openings are evident with both cell types. However, the average current in the lowest trace indicated that the late current is substantially greater in the Δ K1500 mutant. Similar results were obtained in three other patches each. This confirms the enhancement of the late component of Na^+ current in the Δ K1500 mutant channel.

Discussion

We have analyzed the functional effects of the deletion of the positively charged lysine residue at position 1500 in the III/IV interdomain linker of the Na^+ channel α subunit. We were especially interested in this mutation because of the multiple phenotypic effects observed in gene carriers in the affected kindred. Whereas the

Figure 7

Comparison of the late component of Na^+ current in the wild-type and Δ K1500 mutant Na^+ channels. (a and b) The Na^+ current was recorded at high gain (upper trace) and low gain (lower trace) with 200-ms pulses from a holding potential of -100 mV to a test potential of -20 mV. Currents were leakage-subtracted. The dashed lines show the 0 current level. (c) The lowest traces show the average current. The dashed lines indicate the 0 current level. The current calibration refers to the current recorded at high gain (0.15 nA) and low gain (2 nA). The average steady-state current (I_{ss}) is plotted as a function of the peak current ($n = 4$, hH1; $n = 5$, Δ K1500). (d and e) Single-channel currents recorded in cell-attached membrane patches with 200-ms pulses to a test potential of -20 mV with low-resistance microelectrodes. The upper four tracers in each panel show the responses to four consecutive trials.



three-amino acid deletion of the neighboring KPQ sequence was associated with LQTS only, the K1500 deletion also had conduction disturbances as a major phenotypic feature. The EKGs observed in the kindred suggest conduction disturbances at several levels. Our findings can account for the observed phenotypes: (a) Closed-state inactivation rate was enhanced more than tenfold, resulting in a marked reduction of Na⁺ channel availability at the normal resting potential of cardiac cells. Open-state inactivation rate was also increased, but to a lesser extent. The reduction of the Na⁺ current was sufficient to account for the Brugada syndrome and the conduction disturbance at the sinoatrial and alvivo ventricle junctional regions. (b) The late component of Na⁺ current resulting from a return from the inactivated state is increased almost threefold in the ΔK1500 mutant. This late component of Na⁺ current would prolong the action potential duration and the QT interval on the surface EKG, and augment the availability of inward currents (primarily Ca²⁺) required to trigger early and delayed after-depolarizations.

Additional mutations at position 1500 shed light on the function of the interdomain linker in channel gating. The marked negative shift in $V_{1/2h}$ and the reduction of valence corresponding to the loss of $1\epsilon_0$ suggested an electrostatic effect of K1500 on channel inactivation. To clarify such a role, we performed two additional mutations: K1500E, in which the charge at position 1500 is reduced by $2\epsilon_0$, and K1500Q, in which the charge at position 1500 is reduced by $1\epsilon_0$. With both of these mutations, the total number of residues in the III/IV interdomain linker was preserved. To our surprise, the $V_{1/2h}$ was shifted back toward the control value with both the K1500E and the K1500Q mutations. This suggests that it may be the reduction in the number of residues in the segment that accounts for the large negative shift in $V_{1/2h}$. This possibility was supported by the experiments showing a similar negative shift with the ΔK1499 mutant. However, deletion of residues in this region of the molecule may not be equivalent. K1499 and K1500 are contained within a structured α -helical segment of the linker (15). Deletion of K1499 or K1500 may reduce the extended α -helical conformation and increase the mobility of the gate. The three-residue deletion ΔKPQ was not associated with a significant shift in $V_{1/2h}$ (28). These residues are situated 5' to the α -helical segment.

Whereas we observed no relationship between the charge at position 1500 and $V_{1/2h}$, a correlation was observed with the activation parameters $V_{1/2m}$ and k_m . $V_{1/2m}$ was shifted to progressively more positive potentials as the charge was reduced by $1\epsilon_0$ and $2\epsilon_0$. The voltage-dependence of activation was reduced considerably. This suggested an electrostatic interaction between the charge at position 1500 and the activation voltage sensor(s) in the charged S4 residues of each domain. During activation, the S4 segments rotate outward. Repulsion between K1500 and the positive charges of the core of S4 could facilitate the outward

rotation of S4 as activation begins. The decrease in charge of K1500 would reduce this facilitation. Complementary mutation at position 1500 and the cytoplasmic end of S4 might clarify such an effect.

In the wild-type Na⁺ channel, activation and inactivation are coupled. Models of coupling propose that the conformational changes associated with activation, e.g., the outward movement of S4, modulate the receptor for the inactivation gate. Progression along the activation pathway enhances the affinity of the inactivation gate for its receptor. The ΔK1500 mutation appears to uncouple this relationship. From the reduced voltage-dependence and positive voltage shift of activation, one would anticipate a decrease in inactivation rate. Instead, we observed an increase in both closed-state and open-state inactivation rates. The double mutation at the analogous position in the skeletal muscle Na⁺ channel, KK1317/18NN, produced a qualitatively different result. $V_{1/2m}$ and $V_{1/2h}$ were both shifted to depolarized potentials (29).

Relationship to other cardiac Na⁺ channel mutations. The Na⁺ channel α subunit mutations associated with LQTS have a stereotypic functional effect: the late component of Na⁺ current is enhanced. The most common gating defect was a destabilization of the inactivated state, leading to transitions to the open state at late times; another defect that can occur is failure of inactivation, resulting in bursts of opening (4). A less common mechanism was a prolongation of the single-channel open time (30). The functional consequence of the K1500 deletion is more complex. It stabilized the fast-inactivated state. On the other hand, transitions from other states to the channel state associated with failure of inactivation (bursts) or reversibility of inactivation (isolated brief openings) were enhanced. It may be that the increased transition rate into the inactivated state far outweighs a parallel increase in the transition rate out of this state.

The changes in Na⁺ channel function that result in Brugada syndrome and/or progressive conduction system disease are also complex, and in some cases controversial. Some mutations are associated with premature stop codons resulting in the synthesis of nonfunctional proteins. When some mutations, e.g., R1232W/T1620M, were studied in frog oocytes, relatively subtle changes in gating that were unlikely to lead to marked Na⁺ current reduction were observed (2). Changes in gating that resulted from differences in temperature or β subunit modulation were not consistent for the same mutation studied in different laboratories (31, 32). The studies by Chahine and colleagues suggested that the posttranslational processing of the Na⁺ channel is different in oocytes and mammalian cells. Their studies showed that a failure of trafficking of the channel protein might be an important basis for Na⁺ current reduction (6).

Our results with the K1500 deletion are similar to those observed with mutations in other cytoplasmic domains. Bezzina et al. described a kindred with both LQTS and Brugada syndrome associated with the

insertion of an aspartate residue in the carboxy-terminus of the α subunit (1795insD) (33). When expressed in frog oocytes, the mutation was associated with a 7.3-mV negative shift in $V_{1/2h}$, and an 8.1-mV positive shift in $V_{1/2m}$. When expressed in mammalian cells, the 1795insD mutation was associated with a shift in inactivation gating only. Wan et al. described a 6.2-mV positive shift in $V_{1/2m}$, a 1.5-mV reduction in k_m , and an 8.8-mV negative shift in $V_{1/2h}$ in a Brugada syndrome-associated mutation, L567Q (32). This mutation is also located in the I/II cytoplasmic interdomain linker. These studies, and our own of the K1500 deletion, suggest that the cytoplasmic linkers play an important role in activation. Our study is particularly noteworthy in that all three mutations, Δ K1500, K1500E, and K1500Q, are associated with significant reduction in the voltage-dependence of activation. With the K1500E mutation, the activation slope factor is almost doubled. Mutations in S4, a region critical in activation, are usually only associated with parallel shifts in the voltage-dependence of activation.

Patients with other Brugada syndrome-associated mutations are sensitive to Na^+ channel blockers in part because the hyperpolarizing shift in Na^+ channel availability results in a loss of channel availability. We have also observed a similar sensitivity to flecainide in some of the patients with the Δ K1500 mutation. A preliminary analysis suggests that the K1500 deletion increases the fractional block by flecainide compared with the wild-type channel. Viswanathan et al. noted a similar enhancement of tonic block by flecainide of the Na^+ channel mutations 1795insD and Δ KPQ (34). The greater tonic block will make affected individuals more susceptible to flecainide, even at slow heart rates.

It is important to analyze the functional effect of the disease-associated Na^+ channel mutations, despite their large number. Mutations will only cause disease when they affect functionally important domains of the channel protein. They help to identify candidate domains for structure-function studies of this relatively large protein.

Acknowledgments

We wish to express our gratitude to Dianne Mangum for preparation of the manuscript. This was supported by NIH grant RO HL 67145-02.

1. Wang, Q., et al. 1995. SCN5A mutations associated with an inherited cardiac arrhythmia, long QT syndrome. *Cell*. **80**:805–811.
2. Chen, O., et al. 1998. Genetic basis and molecular mechanism for idiopathic ventricular fibrillation. *Nature*. **392**:293–295.
3. Schott, J.-J., Alshinawi, C., and Kyndt, F. 1999. Cardiac conduction defects associate with mutations in SCN5A. *Nat. Genet.* **23**:20–21.
4. Bennett, P.B., Yazawa, K., Makita, N., and George, A.L., Jr. 1995. Molecular mechanism for an inherited cardiac arrhythmia. *Nature*. **376**:683–685.
5. Balsler, J.R. 2001. Inherited sodium channelopathies: novel therapeutic and proarrhythmic molecular mechanisms. *Trends Cardiovasc. Med.* **11**:229–237.
6. Baroudi, G., et al. 2001. Novel mechanism for Brugada syndrome defective surface localization of an SCN5A mutant (R1432G). *Circ. Res.* **88**:E78–E83.

7. Wan, X., Chen, S., Sadeghpour, A., Wang, Q., and Kirsch, G. 2001. Accelerated inactivation in a mutant Na^+ channel associated with idiopathic ventricular fibrillation. *Am. J. Physiol. Heart Circ. Physiol.* **280**:H354–H360.
8. Yan, G.-X., and Antzelevitch, C. 1999. Cellular basis for the Brugada syndrome and other mechanisms of arrhythmogenesis associated with ST-segment elevation. *Circulation*. **100**:1660–1666.
9. Brugada, P., and Brugada, J. 1992. Right bundle branch block, persistent ST segment elevation and sudden cardiac death: a distinct clinical and electrocardiographic syndrome. *J. Am. Coll. Cardiol.* **20**:1391–1396.
10. Tan, H., et al. 2001. A sodium-channel mutation causes isolated cardiac conduction disease. *Nature*. **409**:1043–1047.
11. Bezzina, C., et al. 1999. A single Na^+ channel mutation causing both long-QT and Brugada syndromes. *Circ. Res.* **85**:1206–1213.
12. Veldkamp, M.W., et al. 2000. Two distinct congenital arrhythmias evoked by a multidysfunctional Na^+ channel. *Circ. Res.* **86**:e91–e97.
13. Priori, S.G., et al. 2000. The elusive link between LQT3 and Brugada syndrome. *Circulation*. **102**:945–947.
14. Wattanasirichaigoon, D., et al. 1999. Sodium channel abnormalities are infrequent in patients with long QT syndrome: identification of two novel SCN5A mutations. *Am. J. Med. Genet.* **86**:470–476.
15. Rohl, C.A., et al. 1999. Solution structure of the sodium channel inactivation gate. *Biochemistry*. **38**:855–861.
16. Ming, L., et al. 1993. Convergent regulation of sodium channels by protein kinase C and cAMP-dependent protein kinase. *Science*. **261**:1439–1442.
17. Zhang, L., et al. 2000. Spectrum of ST-T-wave patterns and repolarization parameters in congenital long-QT syndrome. *Circulation*. **102**:2849–2855.
18. Miyazaki, T., et al. 1996. Autonomic and antiarrhythmic drug modulation of ST segment elevation in patients with Brugada syndrome. *J. Am. Coll. Cardiol.* **27**:1061–1070.
19. Higuchi, R. 1990. Recombinant PCR. In *PCR protocols: a guide to methods and applications*. Edited by M.A. Innis, D.H. Gelfand, J.J. Sninsky, and T.J. White, editors. Academic Press Inc. San Diego, California, USA. 177–183.
20. Hamill, O.P., Marty, A., Neher, E., Sakmann, B., and Sigworth, F. 1981. Improved patch-clamp techniques for high-resolution current recording from cell and cell-free membrane patches. *Pflugers Arch.* **391**:85–100.
21. Gilliam, F.R.I., Starmer, C.F., and Grant, A.O. 1989. Blockade of rabbit atrial sodium channels by lidocaine: characterization of continuous and frequency-dependent blocking. *Circ. Res.* **65**:723–739.
22. Grant, A.O., and Starmer, C.F. 1987. Mechanisms of closure of cardiac sodium channels in rabbit ventricular myocytes: single-channel analysis. *Circ. Res.* **60**:897–913.
23. Wang, D.W., Markita, N., Kitabatake, A., Balsler, J.R., and George, A.L., Jr. 2000. Enhanced Na^+ channel intermediate inactivation in Brugada syndrome. *Circ. Res.* **87**:e37–e43.
24. O'Leary, M.E., Chen, L.-Q., Kallen, R.G., and Horn, R. 1995. A molecular link between activation and inactivation of sodium channels. *J. Gen. Physiol.* **106**:641–658.
25. Aldrich, R.W., Corey, D.P., and Stevens, C.F. 1983. A reinterpretation of mammalian sodium channel gating based on single channel recording. *Nature*. **306**:436–441.
26. Aldrich, R.W., and Stevens, C.F. 1983. Inactivation of open and closed sodium channels determined separately. *Cold Spring Harb. Symp. Quant. Biol.* **48**:147–153.
27. Hirschberg, B., Rovner, A., Lieberman, M., and Patlak, J. 1995. Transfer of twelve charges is needed to open skeletal muscle Na^+ channels. *J. Gen. Physiol.* **106**:1053–1068.
28. Chandra, R., Starmer, C.F., and Grant, A.O. 1998. Multiple effects of KPQ deletion mutation on gating of human cardiac Na^+ channels expressed in mammalian cells. *Am. J. Physiol.* **274**:H1643–H1654.
29. Miller, J.R., Patel, M.K., John, J.E., Mounsey, J.P., and Moorman, J.R. 2000. Contributions of charged residues in a cytoplasmic linking region to Na^+ channel gating. *Biochim. Biophys. Acta.* **1509**:275–291.
30. Kambouris, N.G., et al. 1997. Phenotypic characterization of a novel long-QT syndrome mutation (R1623Q) in the cardiac sodium channel. *Circulation*. **97**:640–644.
31. Dumaine, R., et al. 1999. Ionic mechanisms responsible for the electrocardiographic phenotype of the Brugada syndrome are temperature dependent. *Circ. Res.* **85**:803–809.
32. Wan, X., Wang, Q., and Kirsch, G.E. 2000. Functional suppression of sodium channels by B1-subunits as a molecular mechanism of idiopathic ventricular fibrillation. *J. Mol. Cell. Cardiol.* **32**:1873–1884.
33. Bezzina, C., et al. 1999. A single Na^+ channel mutation causing both long-QT and Brugada syndromes. *Circ. Res.* **85**:1206–1213.
34. Viswanathan, P.C., et al. 2001. Gating-dependent mechanisms for flecainide action in SCN5A-linked arrhythmia syndromes. *Circulation*. **104**:1200–1205.